

Dear Author,

Here are the proofs of your article.

- You can submit your corrections **online**, via **e-mail** or by **fax**.
- For **online** submission please insert your corrections in the online correction form. Always indicate the line number to which the correction refers.
- You can also insert your corrections in the proof PDF and **email** the annotated PDF.
- For fax submission, please ensure that your corrections are clearly legible. Use a fine black pen and write the correction in the margin, not too close to the edge of the page.
- Remember to note the **journal title**, **article number**, and **your name** when sending your response via e-mail or fax.
- **Check** the metadata sheet to make sure that the header information, especially author names and the corresponding affiliations are correctly shown.
- **Check** the questions that may have arisen during copy editing and insert your answers/ corrections.
- **Check** that the text is complete and that all figures, tables and their legends are included. Also check the accuracy of special characters, equations, and electronic supplementary material if applicable. If necessary refer to the *Edited manuscript*.
- The publication of inaccurate data such as dosages and units can have serious consequences. Please take particular care that all such details are correct.
- Please **do not** make changes that involve only matters of style. We have generally introduced forms that follow the journal's style. Substantial changes in content, e.g., new results, corrected values, title and authorship are not allowed without the approval of the responsible editor. In such a case, please contact the Editorial Office and return his/her consent together with the proof.
- If we do not receive your corrections **within 48 hours**, we will send you a reminder.
- Your article will be published **Online First** approximately one week after receipt of your corrected proofs. This is the **official first publication** citable with the DOI. **Further changes are, therefore, not possible.**
- The **printed version** will follow in a forthcoming issue.

#### **Please note**

After online publication, subscribers (personal/institutional) to this journal will have access to the complete article via the DOI using the URL: [http://dx.doi.org/\[DOI\]](http://dx.doi.org/[DOI]).

If you would like to know when your article has been published online, take advantage of our free alert service. For registration and further information go to: <http://www.springerlink.com>.

Due to the electronic nature of the procedure, the manuscript and the original figures will only be returned to you on special request. When you return your corrections, please inform us if you would like to have these documents returned.

# Metadata of the article that will be visualized in OnlineFirst

---

ArticleTitle	Co-firing of biomass with coals. 1. Thermogravimetric kinetic analysis of combustion of fir ( <i>abies bornmulleriana</i> ) wood	
--------------	--	--

---

Article Sub-Title		
-------------------	--	--

---

Article CopyRight	Akadémiai Kiadó, Budapest, Hungary (This will be the copyright line in the final PDF)	
-------------------	--	--

---

Journal Name	Journal of Thermal Analysis and Calorimetry	
--------------	---	--

---

Corresponding Author	Family Name	<b>Yürüm</b>
	Particle	
	Given Name	<b>Yuda</b>
	Suffix	
	Division	Faculty of Engineering and Natural Sciences
	Organization	Sabancı University
	Address	Orhanli, Tuzla, Istanbul, 34956, Turkey
	Email	yyurum@sabanciuniv.edu

---

Author	Family Name	<b>Dumanli</b>
	Particle	
	Given Name	<b>Ahu Gümrah</b>
	Suffix	
	Division	Faculty of Engineering and Natural Sciences
	Organization	Sabancı University
	Address	Orhanli, Tuzla, Istanbul, 34956, Turkey
	Email	

---

Author	Family Name	<b>Taş</b>
	Particle	
	Given Name	<b>Sinem</b>
	Suffix	
	Division	Faculty of Engineering and Natural Sciences
	Organization	Sabancı University
	Address	Orhanli, Tuzla, Istanbul, 34956, Turkey
	Email	

---

Schedule	Received	16 September 2010
	Revised	
	Accepted	20 October 2010

---

Abstract	<p>The chemical composition and reactivity of fir (<i>Abies bornmulleriana</i>) wood under non-isothermal thermogravimetric (TG) conditions were studied. Oxidation of the wood sample at temperatures near 600 °C caused the loss of aliphatics from the structure of the wood and created a char heavily containing C–O functionalities and of highly aromatic character. On-line FTIR recordings of the combustion of wood indicated the oxidation of carbonaceous and hydrogen content of the wood and release of some hydrocarbons due to pyrolysis reactions that occurred during combustion of the wood. TG analysis was used to study combustion of fir wood. Non-isothermal TG data were used to evaluate the kinetics of the combustion of this carbonaceous material. The article reports application of Ozawa–Flynn–Wall model to deal with non-isothermal TG data for the evaluation of the activation energy corresponding to the combustion of the fir wood. The average activation energy related to fir wood combustion was 128.9 kJ/mol, and the average reaction order for the combustion of wood was calculated as 0.30.</p>	
----------	--	--

---

Keywords (separated by '-') Co-firing - Combustion - Thermogravimetric analysis - Non-isothermal kinetics - Activation energy of combustion

---

Footnote Information

---

Journal: 10973  
Article: 1126



## Author Query Form

**Please ensure you fill out your response to the queries raised below  
and return this form along with your corrections**

Dear Author

During the process of typesetting your article, the following queries have arisen. Please check your typeset proof carefully against the queries listed below and mark the necessary changes either directly on the proof/online grid or in the 'Author's response' area provided below

<b>Section</b>	<b>Details required</b>	<b>Author's response</b>
Reference	Please check the reference [31].	
Affiliation	Please check and confirm the authors and their respective affiliations are correctly identified and amend if necessary. Please check and confirm the org address.	

## 3 Co-firing of biomass with coals. 1. Thermogravimetric kinetic 4 analysis of combustion of fir (*abies bornmulleriana*) wood

5 Ahu Gümrah Dumanli · Sinem Taş ·  
6 Yuda Yürüm

7 Received: 16 September 2010 / Accepted: 20 October 2010  
8 © Akadémiai Kiadó, Budapest, Hungary 2010

9 **Abstract** The chemical composition and reactivity of fir  
10 (*Abies bornmulleriana*) wood under non-isothermal ther-  
11 mogravimetric (TG) conditions were studied. Oxidation of  
12 the wood sample at temperatures near 600 °C caused the  
13 loss of aliphatics from the structure of the wood and cre-  
14 ated a char heavily containing C–O functionalities and of  
15 highly aromatic character. On-line FTIR recordings of the  
16 combustion of wood indicated the oxidation of carbona-  
17 ceous and hydrogen content of the wood and release of  
18 some hydrocarbons due to pyrolysis reactions that occurred  
19 during combustion of the wood. TG analysis was used to  
20 study combustion of fir wood. Non-isothermal TG data  
21 were used to evaluate the kinetics of the combustion of this  
22 carbonaceous material. The article reports application of  
23 Ozawa–Flynn–Wall model to deal with non-isothermal TG  
24 data for the evaluation of the activation energy corre-  
25 sponding to the combustion of the fir wood. The average  
26 activation energy related to fir wood combustion was  
27 128.9 kJ/mol, and the average reaction order for the com-  
28 bustion of wood was calculated as 0.30.

29  
30 **Keywords** Co-firing · Combustion · Thermogravimetric  
31 analysis · Non-isothermal kinetics · Activation energy of  
32 combustion

### 33 Introduction

34 Biomass (wood, agricultural residues, forestry residues,  
35 energy crops, etc.) is a renewable fuel and the fourth largest

following coal, oil, and natural gas [1]. Compared with 36  
fossil fuels, biomass has the advantages of being harmless 37  
in regard to the emissions of carbon dioxide, as this par- 38  
ticipates in biomass growth through the photosynthesis 39  
reactions, and reducing pollutant species generation, given 40  
the low sulfur and nitrogen contents. From an economic 41  
point of view, the possibility of co-firing of biomass with 42  
coal in power plants can be an interesting alternative, since 43  
it allows for the use of existing infrastructures already 44  
equipped with proper devices for emission control, reduc- 45  
ing simultaneously fossil fuels consumption [2]. Informa- 46  
tion of the chemical composition and reactivity of the 47  
biomass, the thermal phenomena occurring during solid 48  
fuels combustion is very important for the effective oper- 49  
ation of conversion units. 50

Thermal analysis methods have been extensively used 51  
in recent years, because they offer a quick quantitative tech- 52  
nique for the assessment of pyrolysis or combustion pro- 53  
cesses under non-isothermal conditions and allow to guess 54  
the effective kinetic parameters for the various decompo- 55  
sition reactions [3–13]. Kinetics of coal-biomass combus- 56  
tion has been investigated by many research groups 57  
recently [14–17]. 58

The reaction kinetics parameters of combustion of wood 59  
under differential oxidizing conditions were calculated 60  
with the method given in Sanchez et al. [18] as follows. 61  
The rate of heterogeneous solid-state reactions can gener- 62  
ally be explained by 63

$$\frac{d\alpha}{dt} = k(T) f(\alpha) \quad (1)$$

where  $t$  is time,  $k(T)$  the temperature-dependent constant, 65  
and  $f(\alpha)$  a function described the reaction model, which 66  
expresses the dependence of the reaction rate on the extent 67  
of reaction,  $\alpha$ . The temperature dependence of the rate 68

A1 A. G. Dumanli · S. Taş · Y. Yürüm (✉)  
A2 Faculty of Engineering and Natural Sciences, Sabanci  
A3 University, Orhanli, Tuzla, Istanbul 34956, Turkey  
A4 e-mail: yyurum@sabanciuniv.edu

69 constant is explained by the Arrhenius equation. Thus, the  
70 rate of a solid-state reaction can generally be illustrated by

$$\frac{d\alpha}{dt} = Ae^{-\frac{E}{RT}} f(\alpha) \quad (2)$$

72 where  $A$  is the pre-exponential Arrhenius factor,  $E$  the  
73 activation energy, and  $R$  the gas constant.

74 For dynamic data obtained at a constant heating rate

$$\beta = \frac{dT}{dt} = \text{constant}$$

76 this term is inserted in Eq. 2 so the above rate expression  
77 can be converted into non-isothermal rate expressions  
78 describing reaction rates as a function of temperature at a  
79 constant  $\beta$ .

$$\frac{d\alpha}{dT} = \frac{1}{\beta} Ae^{-\frac{E}{RT}} f(\alpha) \quad (3)$$

81 Integrating up to conversion,  $\alpha$ , Eq. 3 gives,

$$\int_0^\alpha \frac{d\alpha}{f(\alpha)} = g(\alpha) = \frac{A}{\beta} \int_{T_0}^T e^{-\frac{E}{RT}} dT \quad (4)$$

83 Isoconversional methods include carrying out a series of  
84 experiments at different heating rates [19, 20]. In this study,  
85 activation energies from dynamic data were obtained from  
86 isoconversional method by Ozawa [21, 22], Flynn and Wall  
87 [23] using the Doyle's approximation of  $p(x)$  [24], which  
88 involves measuring the temperatures corresponding to fixed  
89 values of  $\alpha$  from experiments at different heating rates.

$$\ln(\beta) = \ln \left[ \frac{AE}{Rg(\alpha)} \right] - 5331 - 1052 \frac{E}{RT} \quad (5)$$

91 From this equation, the activation energy  $E$  may be  
92 estimated by plotting  $\ln(\beta)$  versus  $1/T$ .

93 To find out the reaction order, Avrami's theory [25–27]  
94 was used to describe non-isothermal cases, where variation  
95 of the degree of conversion with temperature and heating  
96 rate can be explained as

$$\alpha(T) = 1 - \exp \left[ -\frac{k(T)}{\beta^n} \right] \quad (6)$$

98 Taking the double natural logarithm of both sides of  
99 Eq. 6, with  $k(T) = Ae^{-E/RT}$ , yields

$$\ln[-\ln(1 - \alpha(T))] = \ln A - \frac{E}{RT} - n \ln \beta \quad (7)$$

101 Therefore, a plot of  $\ln[-\ln(1 - \alpha(T))]$  versus  $\ln \beta$ , which  
102 is obtained at the same temperature from a number of  
103 isotherms taken at different heating rates, should give in  
104 straight lines whose slope will have the value of the  
105 reaction order or the Flynn–Wall–Ozawa exponent  $n$  [21,  
106 28]. Extra aspects of the technique applied to examine the  
107 process are explained by Ozawa [22].

The aim of this study was to determine the chemical  
composition and reactivity of fir wood under non-isothermal  
thermogravimetric (TG) conditions. This study provided a  
kinetic evaluation of the combustion of fir wood. The Ozawa–  
Flynn–Wall model was used to deal with non-isothermal TG  
data to calculate the activation energy of the fir wood  
combustion. The data obtained will be useful to understand  
the behavior of fir wood during combustion. The information  
obtained will be used in the co-firing of the wood with low  
rank Turkish coals.

## Experimental

### Materials and characterization

The fir wood sample used in this study was a bark-free fir  
(*Abies bornmulleriana*) sawdust sample obtained from Bolu  
forests (northwest Anatolia) in Turkey. The proximate and  
elemental analyses of the wood sample were done at the  
Instrumental Analysis Laboratory of the Scientific and Technical  
Research Council of Turkey, Ankara, is given in Table 1. The  
sawdust was ground and sieved to below 175  $\mu\text{m}$  (–80 mesh)  
size. Wood sample was characterized in terms of proximate  
analysis according to the ASTM standards (ASTM E871, ASTM  
D1102-84, ASTM D3172-89) using laboratory furnaces, ultimate  
analysis using CHN-600 and S532-500 analyzers (ASTM  
D3176-93, ASTM D3177-33). Calorific values of the samples  
were determined with a Parr 6100 calorimeter according to  
ASTM D2015-95 in our laboratories.

### Thermogravimetric analysis

Wood combustion tests were performed in a Netzsch STA  
449 C Jupiter differential thermogravimetric analyzer (precision  
of temperature measurement  $\pm 2$  °C, microbalance sensitivity  
 $< 5$   $\mu\text{g}$ ), with which the sample weight loss

**Table 1** Proximate and elemental analyses of fir wood

Proximate analysis/% (as received)	
Volatile matter	85.5
Fixed carbon	10.5
Moisture	3.7
Ash	0.3
Elemental analysis/% (daf)	
Carbon	47.2
Hydrogen	6.1
Nitrogen	0.3
Oxygen (by difference)	46.7
H/C (atomic)	1.55

140 and rate of weight loss as functions of time or temperature  
 141 were recorded continuously, under dynamic conditions, in  
 142 the range 25–1000 °C. The experiments were carried out  
 143 under an air atmosphere, with a flow rate of 60 mL/min,  
 144 and combustion of the samples was performed in the fur-  
 145 nace of the thermobalance under controlled temperature to  
 146 obtain the corresponding TG curves with heating rates ( $\beta$ )  
 147 of 5, 10, 20, and 30 °C/min as it was also conducted in  
 148 current literature [29, 30]. Preliminary tests with different  
 149 sample masses and sizes and gas flow rates were carried  
 150 out, to check the influence of heat and mass transfer.  
 151 20–25 mg of each material, of  $\sim 250$   $\mu\text{m}$  particle size, was  
 152 found to be optimum to eliminate the effects of eventual  
 153 side reactions and mass and heat transfer limitations, was  
 154 thinly distributed in the crucible in the experiments. The  
 155 experiments were replicated at least twice to determine  
 156 their reproducibility, which was found to be satisfactory.

157 The TG–FTIR runs were carried out in a Netzsch STA  
 158 449 C Jupiter TG system coupled to a Bruker Equinox 55  
 159 FTIR spectrometer under a dynamic air atmosphere. TG  
 160 analysis was done from 25 to 1000 °C at a linear heating  
 161 rate of 10 °C/min. The output of the TGA system was  
 162 connected to the FTIR spectrometer through a heated line.  
 163 The balance adapter, the transfer line, and the FTIR gas  
 164 cell can be heated until 250 °C, thus avoiding the con-  
 165 densation of the less volatile compounds. On the other  
 166 hand, the low volumes in the thermobalance microfurnace,  
 167 transfer line, and gas measurement cell permit low carrier  
 168 gas flow rates to be used and allow for good detection of  
 169 the gases evolved in the pyrolysis process. In all the  
 170 experiments, the transfer line and the gas measurement cell  
 171 were maintained at 200 °C. Online gas analyses were  
 172 performed for the detection of combustion gases fed to  
 173 FTIR spectrometer, and experimental data were stored as a  
 174 function of time.

## 175 FTIR spectra

176 FTIR spectra of the original and fir wood samples oxidized  
 177 under an air atmosphere at 200, 300, 350, 380, 400, 500,  
 178 and 600 °C were obtained using a Bruker Equinox 55 FTIR  
 179 spectrometer equipped with an ATR system by co-adding  
 180 20 scans over the range 600–4000  $\text{cm}^{-1}$  performed at  
 181 1  $\text{cm}^{-1}$  of digital resolution. The assignment of the bands  
 182 in the FTIR spectra was according to Shevla [31].

## 183 Scanning electron microscopy

184 Morphology of the wood and its ashes was examined by  
 185 scanning electron microscopy. Leo Supra 35VP Field  
 186 emission scanning electron microscope (SEM), Leo 32 and  
 187 energy dispersive X-ray spectrometer (EDS) were used for  
 188 images and analyses of the major ash-forming elements in

189 different ashes. Wood and ash samples were mounted on  
 190 stubs and gold-coated before analysis, to make them  
 191 electrically conductive. Imaging was generally done at  
 192 2–5 keV accelerating voltage, using the secondary electron  
 193 imaging technique.

## 194 Results and discussion

### 195 SEM–EDS analysis

196 Morphology of the wood and its ash obtained at 900 °C  
 197 was investigated by SEM, Fig. 1. Physical appearances of  
 198 wood and its ashes were quite different. The SEM photo-  
 199 graphs indicated that these contained material with diverse  
 200 morphology. While micro structure of the wood contained  
 201 amorphous, the ash was consisted of some prismatic,  
 202 mainly micron-scale cubical forms of 0.2  $\mu\text{m}$  size. EDS  
 203 analysis of the wood ash revealed, Table 2, that the ash  
 204 contained unburned carbon and in the order of decreasing  
 205 percentage oxides of calcium, aluminum, potassium,  
 206 magnesium, and sodium. Ash elements can exert a catalytic



Fig. 1 SEM micrographs of a fir wood and b residue of fir wood fired at 900 °C



**Table 2** EDS analysis results of the ash obtained at 900 °C

Element	Series	Net	Unnor. wt%	Norm. wt%	At.%
Carbon	K series	293	5.9456	5.2861	10.3084
Oxygen	K series	2458	39.9036	35.4771	51.9369
Magnesium	K series	164	1.2457	1.1075	1.0673
Calcium	K series	305	43.7126	38.8635	22.7127
Sodium	K series	76	0.5506	0.4895	0.4987
Aluminum	K series	1035	9.3138	8.2806	7.1883
Potassium	K series	197	11.8048	10.4953	6.2874

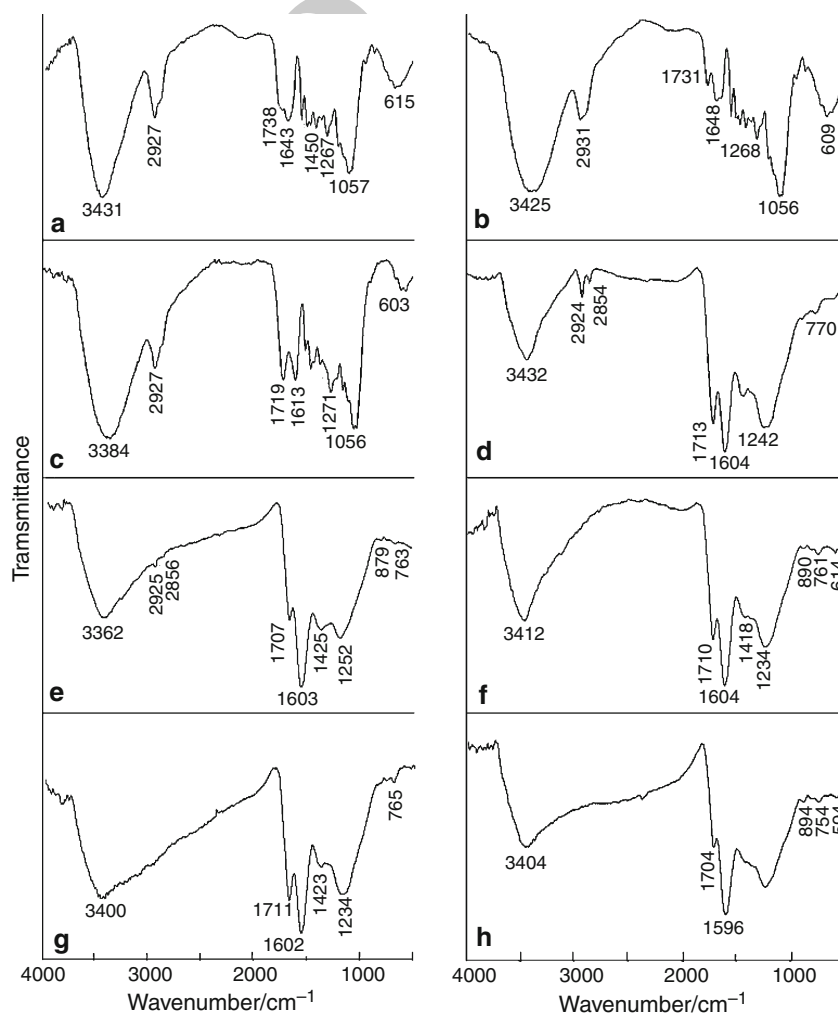
207 role on the reactivity of organic material during combustion of the wood. Karabakan and Yürüm [32] found that  
 208 mainly carbonates of calcium and magnesium have a mild  
 209 effect to promote the oxidation organic material in carbo-  
 210 naceous fuels.  
 211

212 FTIR analysis of the original and oxidized fir wood

213 FTIR spectra recorded in the 400–4000  $\text{cm}^{-1}$  region of  
 214 original fir wood and oxidized fir wood are presented in

Fig. 2. FTIR spectrum of the wood, Fig. 2a, contained a strong broad O–H stretching at 3300–4000  $\text{cm}^{-1}$ , C–H stretching at 2800–3000  $\text{cm}^{-1}$ , and several distinct peaks in the finger print region between 500 and 1750  $\text{cm}^{-1}$ . Most of these bands have contribution from both carbohydrates (cellulose and hemicellulose) and lignin. More specifically, the bands at 3431 and 1450  $\text{cm}^{-1}$  (characteristic of hydrogen bonded OH groups), 2927 and 1470  $\text{cm}^{-1}$  (C–H stretching of methyl or methylene groups) [31]. The band at 1738  $\text{cm}^{-1}$  in the spectrum of the wood is due to uranic acid and acetyl groups in the hemicellulosic material of the wood [33]. The presence of a sharp signal at 1643  $\text{cm}^{-1}$  can be attributed to the aromatic rings in quinonic structures. Specific band maxima in 1260–1000  $\text{cm}^{-1}$  regions were related with ring vibrations overlapped with stretching vibrations of (C–OH) side groups and the (C–O–C) glycosidic bond vibration, typical of xylans. Bands at 1267 and 1057  $\text{cm}^{-1}$  are indicative of hemicelluloses. Bands in the range of 1270–1050  $\text{cm}^{-1}$  belong to C–O and C–O–C groups [33].

**Fig. 2** FTIR spectra of  
 a original fir wood and fir wood  
 oxidized at b 200 °C, c 300 °C,  
 d 350 °C, e 380 °C, f 400 °C,  
 g 500 °C, and h 600 °C





236 The FTIR spectra of the wood oxidized at 200, 300, 350,  
 237 380, 400, 500, and 600 °C are presented between Fig. 2b  
 238 and h, respectively. The significant change in the spectra of  
 239 oxidized wood seemed in the intensity of C–H stretching of  
 240 methyl or methylene peaks in the zone 2930–2924  $\text{cm}^{-1}$ ,  
 241 decreased steadily until 380 °C and beyond this tempera-  
 242 ture these functionalities appeared to be lost. The other  
 243 significant change was the nascence of new absorption  
 244 bands due to oxygenated functions such as C–O distin-  
 245 guished in the zone of 1731 and 1704  $\text{cm}^{-1}$ . As the oxi-  
 246 dation temperature was increased from 300 to 600 °C  
 247 intensity of the C–O band increased and the peaks shifted  
 248 from 1731 to 1704  $\text{cm}^{-1}$  strongly suggesting a rearrange-  
 249 ment among the C–O functionalities during oxidation, the  
 250 1734  $\text{cm}^{-1}$  band is characteristic of non-conjugated car-  
 251 bonyl group [34]. The third important change was sharp  
 252 increase in the intensity of the absorption bands due to  
 253 aromatic ring breathing vibrations near 1600  $\text{cm}^{-1}$ , indi-  
 254 cating the formation of a product of high aromaticity.  
 255 Therefore, oxidation of the wood sample at temperatures  
 256 near 600 °C caused the loss of aliphatics from the structure  
 257 of the wood and created a char heavily containing C–O  
 258 functionalities and of highly aromatic character.

### 259 TG–FTIR experiments

260 The evolution of gaseous species and products as a result of  
 261 the oxidation of wood sample was simultaneously moni-  
 262 tored by FTIR during the TG experiment at the heating rate  
 263 of 10 °C/min. The FTIR spectra of the gases evolved  
 264 during are presented in Fig. 3. The spectra were detected at  
 265 increasing times, and the corresponding temperatures at  
 266 which the spectra were recorded are denoted on the spectra.  
 267 Spectra indicated the nascence and development of certain

268 peaks. Bernstein et al. [35] who investigated the infrared  
 269 spectra of  $\text{CO}_2$  indicated the following peaks were due to  
 270  $\text{CO}_2$ : 3720, 3600, 3300, 2375, 1620, 750, and 675  $\text{cm}^{-1}$ .  
 271 Lemus [36] who studied on infrared spectra of water vapor  
 272 showed that the peaks at 3756, 3657, and 1594  $\text{cm}^{-1}$  were  
 273 due to water vapor. Spectra recorded in this study con-  
 274 tained the following peaks: 3720, 3563, 2375, and  
 275 1688  $\text{cm}^{-1}$  due to  $\text{CO}_2$ , 3188 [37] and 1550  $\text{cm}^{-1}$  due to  
 276 water vapor, and 844  $\text{cm}^{-1}$  due to hydrocarbons. The large  
 277 peak at 3188  $\text{cm}^{-1}$  in the spectrum obtained in the 2833rd  
 278 second that was due to water vapor indicated the combu-  
 279 sion of hydrogen content of the wood, that was also an  
 280 indication of high hydrogen content of the wood ( $\text{H}/$   
 281  $\text{C} = 1.55$ ). On-line FTIR recordings of the combustion of  
 282 wood indicated the oxidation of carbonaceous and hydro-  
 283 gen content of the wood and release of some hydrocarbons  
 284 due to pyrolysis reactions that occurred during combustion  
 285 of the wood.

### Heat treatment of wood under oxidative and non-oxidative atmospheres

288 In this study, the wood sample was subjected to heat  
 289 treatment at different temperatures between 100 and  
 290 400 °C in the presence of air. The mass loss according to  
 291 the heat treatment was recorded, and calorific values of the  
 292 samples were measured using an adiabatic calorimeter. The  
 293 results were compared with the untreated wood sample.  
 294 Results are shown in Table 3. According to the calorific  
 295 value results, during the heat treatment of the wood sample  
 296 under an air atmosphere, up to 200 °C the calorific value of  
 297 the wood increased from 18746 to 19521 kJ/kg due to the  
 298 removal of the low volatile compounds. As the heat  
 299 treatment temperature was increased to 300 °C and higher

**Fig. 3** TGA–FTIR spectra of gases released during combustion of fir wood heated under a dynamic air atmosphere from 25 to 1000 °C by a heating rate of 10 °C/min

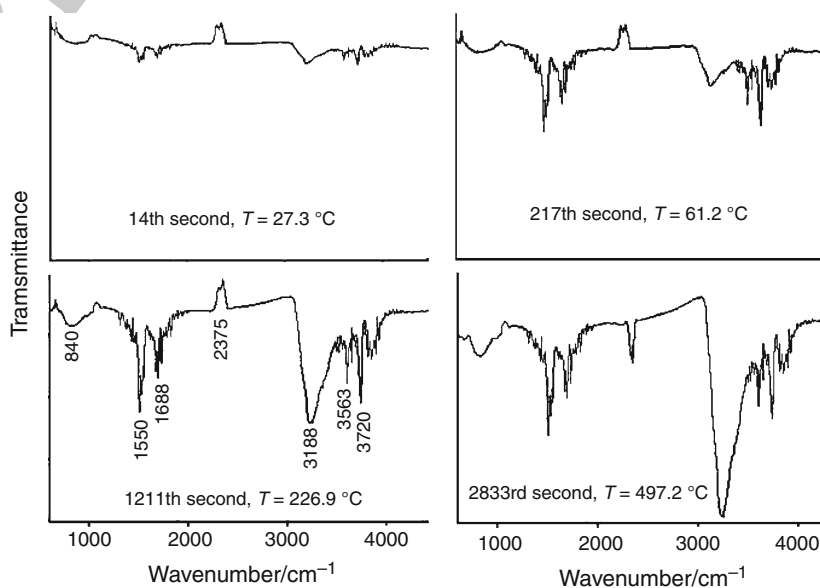


**Table 3** Effect of heat treatment under an air atmosphere on the calorific values of the wood

Heat treatment temperature/°C	Mass loss/%	Calorific value/kJ/kg
Unheated	–	18746
100	5.9	19135
200	11.0	19521
300	32.0	3149
400	99.3	–

**Table 4** Effect of heat treatment under an argon atmosphere on the calorific values of the wood

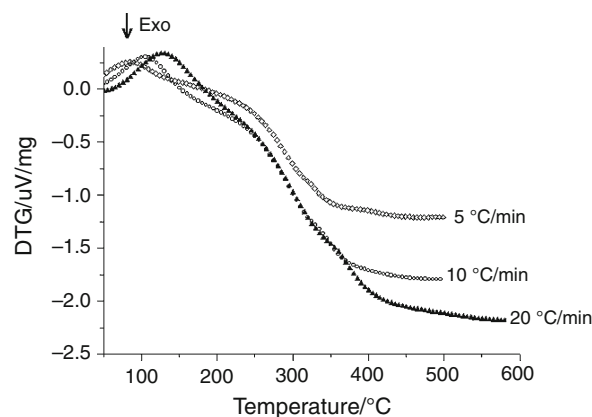
Heat treatment temperature/°C	Mass loss/%	Calorific value/kJ/kg
Unheated	–	18746
100	10.1	19001
200	11.7	19910
300	27.0	24210
400	97.1	–

300 temperatures, parallel to the pyrolytic losses of carbonaceous material from the structure of the wood and combustion of the carbonaceous material the calorific values decreased sharply to 3149 kJ/kg.

304 The same experiment was repeated under an argon atmosphere, and the results are shown in Table 4. In these experiments, the calorific values steadily increased from 18746 to 24210 kJ/kg due to the removal of volatiles producing residual matter rich in carbon. Further increase of the temperature volatilized all the carbonaceous material. The TG experiments gave information of the percent material loss during heat treatment.

### 312 TG experiments

313 This study on reactivity of wood, useful for kinetic analysis, was mainly based on TG measurements. DTG tracings obtained during the oxidation of wood with different heating rates were presented in Fig. 4. The TG curves measured from the temperature programmed combustion of the wood samples at the heating rates ( $\beta$ ) of 5, 10, 20, and 30 °C/min were illustrated in Fig. 5. As it might be examined, on raising the temperature, combustion of the sample occurred with a related mass loss. Once the fuel content of the wood was consumed, the mass corresponding to the ashes stayed constant. Given the small sample amounts and the relatively slow heating rates, the weight loss versus temperature curves showed several sequential zones, as in the example for wood exposed to air. The weight loss versus temperature curves showed several

**Fig. 4** DTG tracings obtained during the oxidation of wood with different heating rates

328 sequential zones, as in the example for wood exposed to 328  
329 air. The first zone of weight loss, temperatures below 329  
330 390 °C and conversion up to 60%, was the pyrolysis (or 330  
331 devolatilization) stage, whose characteristics were affected 331  
332 by the presence of oxygen in the reaction environment. 332  
333 Char oxidation, adjoining solid pyrolysis, was completed at 333  
334 about 875 °C. 334

335 Figure 5 shows the TG mass loss curve of the wood with 335  
336 at various heating rates ( $\beta$ ) (5, 10, 20, and 30 K/min) to 336  
337 study the effect of heating rate on non-isothermal kinetics. 337  
338 There were two main temperatures for mass losses for 338  
339 every heating rate (Fig. 5). The first temperature range was 339  
340 339.2–381.1 °C; as the heating rate was increased the 340  
341 greater mass losses were detected at higher temperatures. 341  
342 The second temperature range at which more material loss 342  
343 occurred was 537.9–875.7 °C; in this range, higher heating 343  
344 rates caused higher losses at more elevated temperatures. 344  
345 Residual masses in the range of 1.01–2.24% were obtained 345  
346 at about 1009–1019 °C. So there were several steps for 346  
347 mass losses; at 95 °C humidity of the wood was lost, 347  
348 depending on the heating rate at about 340–380 °C, 348  
349 56–62% of the volatiles were lost and in the temperature 349  
350 range of 540–875 °C the total material loss reached to 350  
351 96–98%. Higher heating rates caused higher material loss 351  
352 compared to the loss of material at lower heating rates. 352  
353 Since small masses of wood (20–25 mg) were utilized in 353  
354 each experiment, and particle size of the wood was reduced 354  
355 to <250  $\mu$ m, mass and heat transfer limitations were 355  
356 eliminated. The data obtained using different heating rates 356  
357 during firing experiments, therefore, did not contain any 357  
358 restrictive resistances. As the heating rate was increased, 358  
359 the maximum mass loss and/or maximum rate of combustion 359  
360 shifted to higher temperatures. This was attributed to the 360  
361 changes in the rate of heat transfer with the increase 361  
362 in the heating rate and the short exposure time to a particular 362  
363 temperature at high heating rates, as well as the 363  
364 effect of the kinetics of combustion. 364

**Fig. 5** TG tracings obtained during the oxidation of wood with different heating rates in the temperature range of 25–1000 °C

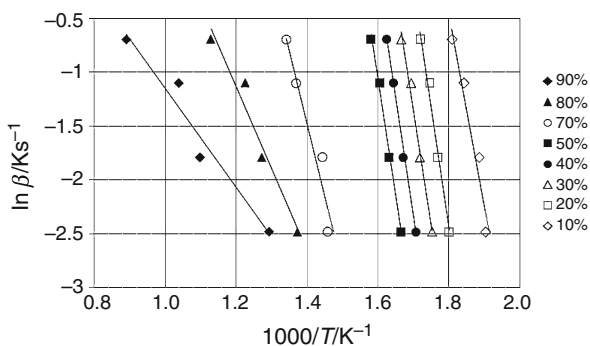
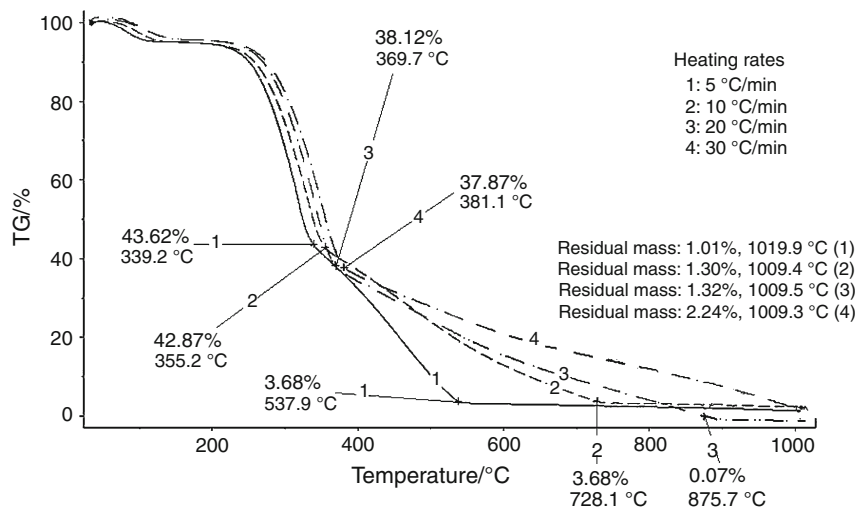


**Fig. 6** Curves of fitting to kinetic model proposed by Ozawa–Flynn–Wall to various conversion percentages corresponding to the combustion of fir wood at different heating rates for the calculation of activation energies

365 Eight different percentages of conversion ( $\alpha$ ) are pointed  
 366 out in each curve in Fig. 5: 10, 20, 30, 40, 50, 70, 80,  
 367 and 90%. The plots of  $\ln \beta$  versus  $1/T$  corresponding to the  
 368 several conversion degrees of the process were shown in

Fig. 6 for wood. Generally, there were linear relations for 369  
 the conversion percentages so the activation energies were 370  
 calculated from the corresponding slopes according to the 371  
 Ozawa–Flynn–Wall kinetic method, Table 5. Raising the 372  
 temperature, combustion of the sample occurred with mass 373  
 losses and related decrease in activation energies. Activa- 374  
 tion energy calculated at 10% conversion was 142.3 kJ/mol 375  
 and steadily increased until 50% conversion to a value of 376  
 169.8 kJ/mol then as the material loss increased beyond 377  
 this point, the activation energy started to decrease until 378  
 36.4 kJ/mol at conversion of 90%. It seemed that the first 379  
 phase of reactions constituted the rate determining set of 380  
 reactions with average activation energy of 165.8 kJ/mol. 381  
 Beyond 70% conversion in combustion reactions, the 382  
 average activation energy dropped to 67.6 kJ/mol. The 383  
 overall average activation energy of the combustion of 384  
 the wood was calculated to be 128.9 kJ/mol. This value 385  
 calculated for fir wood seemed to be higher than those, 386  
 54–92 kJ/mol, calculated by Kök [38] for some Turkish 387

**Table 5** Slopes and correlation coefficients ( $R^2$ ) corresponding to linear fittings to kinetic model proposed by Ozawa–Flynn–Wall to various conversion percentages corresponding to the combustion of wood at different heating rates together with the resultant activation energy ( $E$ ) values

Conversion/%	$R^2$	Slope	Activation energy/kJ/mol	Average activation energy/kJ/mol	
10	0.953	-18.01	142.3	Rate determining phase 165.8	
20	0.987	-22.51	177.9		
30	0.988	-21.07	166.5		
40	0.997	-21.83	172.5		
50	0.993	-21.48	169.8		
70	0.936	-13.44	106.2		Fast reactions 67.6
80	0.959	-7.61	60.1		
90	0.951	-4.61	36.4		
Overall average activation energy/kJ/mol				128.9	

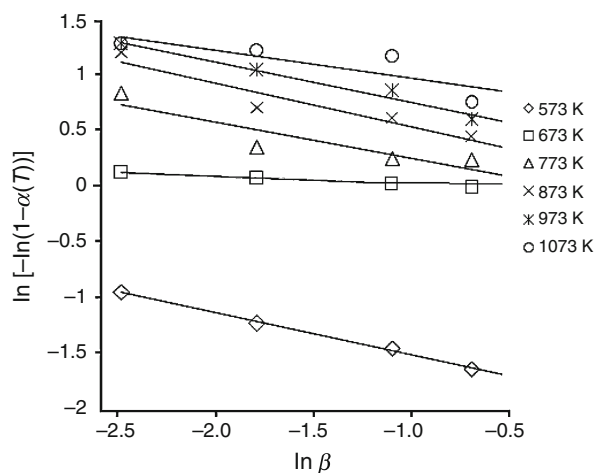


**Fig. 7** Straight lines fitting to Ozawa–Flynn–Wall kinetic model for various conversion percentages corresponding to the combustion of wood at different heating rates for the determination of reaction order  $n$

**Table 6** Reaction order ( $n$ ) as a function of temperature for the combustion of wood

$T/^\circ\text{C}$	Reaction order/ $n$
300	0.38
400	0.10
500	0.32
600	0.39
700	0.36
800	0.25
Average $n$	0.30

low rank coals using Coats and Redfern method [39], but lower than those calculated for the combustion of biomass using the Ozawa–Flynn–Wall kinetic method, 140 kJ/mol [18]. Otero et al. [40] using the Ozawa–Flynn–Wall kinetic method with a semianthracite coal calculated the average activation energy of combustion as 67.3 kJ/mol.

For the computation of the reaction order, the plots of  $\ln[-\ln(1 - \alpha(T))]$  versus  $\ln \beta$  have been represented in Fig. 7. The  $n$  values as a function of temperature for wood combustion are shown in Table 6. The values changed from very close to zero to around 0.3 and are dependent on the extent of the reaction, i.e., not constant during the reaction, which was an evidence of the multiple step processes such as devolatilization and combustion. The lowest value for  $n$  was measured at 400 °C at which the slope of the % TG versus temperature curves changed sharply indicating a change in the combustion regime. After this temperature, the order of the reaction again raised to values close to the average value of 0.30.

## Conclusions

EDS analysis of the wood ash revealed that the ash contained unburned carbon and in the order of decreasing percentage oxides of calcium, aluminum, potassium, magnesium, and sodium. Oxidation of the wood sample at temperatures near 600 °C caused the loss of aliphatics from the structure of the wood and created a char heavily containing C–O functionalities and of highly aromatic character. On-line FTIR recordings of the combustion of wood indicated the oxidation of carbonaceous and hydrogen content of the wood and release of some hydrocarbons due to pyrolysis reactions that occurred during combustion of the wood. Heat treatment of the wood sample under an air atmosphere, up to 200 °C, caused the calorific value of the wood to increase from 18746 to 19521 kJ/kg due to the removal of the low volatile compounds. As the heat treatment temperature was increased to 300 °C and higher temperatures, parallel to the pyrolytic losses of carbonaceous material from the structure of the wood and combustion of the carbonaceous material the calorific values decreased sharply to 3149 kJ/kg. The weight loss versus temperature curves showed several sequential zones, as in the example for wood exposed to air. The first zone of weight loss, temperatures below 390 °C and conversion up to 60%, was the pyrolysis (or devolatilization) stage, whose characteristics were affected by the presence of oxygen in the reaction environment. Char oxidation, adjoining solid pyrolysis, was completed at about 875 °C. It seemed that the first phase of reactions constituted the rate determining set of reactions with average activation energy of 165.8 kJ/mol. Beyond 70% conversion in combustion reactions, the average activation energy dropped to 67.6 kJ/mol. The overall average activation energy of the combustion of the wood was calculated to be 128.9 kJ/mol. The value of order of reaction changed from very close to zero to around 0.3 and are dependent on the extent of the reaction, i.e., not constant during the reaction, which was an evidence of the multiple step processes.

## References

- Di Blasi C. Combustion and gasification rates of lignocellulosic chars. *Progress Energy Comb Sci.* 2009;35:121–40.
- Vamvuka D, Salpigidou N, Kastanaki E, Sfakiotakis S. Possibility of using paper sludge in co-firing applications. *Fuel.* 2009; 88:637–43.
- Várhegyi G, Szabó P, Jakab E, Till F. Mathematical modeling of char reactivity in Ar-O<sub>2</sub> and CO<sub>2</sub>-O<sub>2</sub> mixtures. *Energ Fuels.* 1996;10:1208–14.
- Ceylan K, Karaca H, Önal Y. Thermogravimetric analysis of pretreated Turkish lignites. *Fuel.* 1999;78:1109–16.



- 457 5. Adánez J, De Diego LF, García-Labiano F, Abad A, Abanades  
458 JC. Determination of biomass char combustion reactivities for fbc  
459 applications by a combined method. *Ind Eng Chem Res.* 2001;40:4317–23.  
460
- 461 6. Otero M, Díez C, Calvo LF, García AI, Mordu A. Analysis of the  
462 co-combustion of sewage sludge and coal by TG-MS. *Biomass*  
463 *Bioenerg.* 2002;22:319–29.  
464
- 465 7. Quanrum L, Haoquan H, Qiang Z, Shengwei Z, Gouohua C.  
466 Effect of inorganic matter on reactivity and kinetics of coal  
467 pyrolysis. *Fuel.* 2004;83:713–8.  
468
- 469 8. Mianowski A, Bigda R, Zymła V. Study on kinetics of com-  
470 bustion of brick-shaped carbonaceous materials. *J Therm Anal*  
471 *Calorim.* 2006;84:563–74.  
472
- 473 9. Franceschi E, Cascone I, Nole D. Thermal, XRD and spectro-  
474 photometric study on artificially degraded woods. *J Therm Anal*  
475 *Calorim.* 2008;91:119–25.  
476
- 477 10. Xu Q, Griffin GJ, Jiang Y, Preston C, Bicknell AD GP, Bradbury  
478 GP, White N. Study of burning behavior of small scale wood crib  
479 with cone calorimeter. *J Therm Anal Calorim.* 2008;91:787–90.  
480
- 481 11. Yu LJ, Wang S, Jiang XM, Wang N, Zhang CQ. Thermal anal-  
482 ysis studies on combustion characteristics of seaweed. *J Therm*  
483 *Anal Calorim.* 2008;93:611–7.  
484
- 485 12. Otero M, Gómez X, García AI, Morán A. Non-isothermal ther-  
486 mogravimetric analysis of the combustion of two different car-  
487 bonaceous materials coal and sewage sludge. *J Therm Anal*  
488 *Calorim.* 2008;93:619–26.  
489
- 490 13. Suarez AC, Tancredi N, Cesar P, Pinheiro C, Yoshida MI.  
491 Thermal analysis of the combustion of charcoals from Eucalyptus  
492 dunnii obtained at different pyrolysis temperatures. *J Therm Anal*  
493 *Calorim.* 2010;100:1051–4.  
494
- 495 14. Kastanaki E, Vamvuka D. A comparative reactivity and kinetic  
496 study on the combustion of coal–biomass char blends. *Fuel.*  
497 2006;85:1186–93.  
498
- 499 15. Gil MV, Casal D, Pevida C, Pis JJ, Rubiera F. Thermal behaviour  
500 and kinetics of coal/biomass blends during co-combustion. *Bi-*  
501 *oresour Technol.* 2010;101:5601–8.  
502
- 503 16. Muthuraman M, Namioka T, Yoshikawa K. Characteristics of co-  
504 combustion and kinetic study on hydrothermally treated munic-  
505 ipal solid waste with different rank coals: A thermogravimetric  
506 analysis. *Appl Energ.* 2010;87:141–8.  
507
- 508 17. Sahu SG, Sarkar P, Chakraborty N, Adak AK. Thermogravi-  
509 metric assessment of combustion characteristics of blends of a  
coal with different biomass chars. *Fuel Process Technol.* 2010;  
91:369–78.
18. Sanchez ME, Otero M, Gomez X, Moran A. Thermogravimetric  
kinetic analysis of the combustion of biowastes. *Renew Energ.*  
2009;34:1622–7.
19. Vyazovkin S. Evaluation of activation energy of thermally  
stimulated solid-state reactions under arbitrary variation of tem-  
perature. *J Comput Chem.* 1997;18:393–402.
20. Khawam A, Flanagan DR. Role of isoconversional methods in  
varying activation energies of solid-state kinetics: II. Noniso-  
thermal kinetic studies. *Thermochim Acta.* 2005;436:101–12.
21. Ozawa T. A new method of analyzing thermogravimetric data. *Bull Chem Soc Jpn.* 1965;38:1881–6.
22. Ozawa T. Kinetic analysis of derivative curves in thermal anal-  
ysis. *Therm Anal.* 1970;2:301–24.
23. Flynn JH, Wall LA. Structures and thermal analysis of 1,1,6,6-  
tetraphenylhexa-2,4-diyne-1,6-diol. *Polym Lett.* 1966;4:323–8.
24. Doyle CD. Estimating isothermal life from thermogravimetric  
data. *J Appl Polym Sci.* 1962;6:639–42.
25. Avrami MJ. Kinetics of phase change. I. General theory. *Chem*  
*Phys.* 1939;7:1103–12.
26. Avrami MJ. Kinetics of phase change. II. Transformation-time  
relations for random distribution of nuclei. *Chem Phys.* 1940;8:  
212–24.
27. Avrami MJ. Kinetics of phase change. III. Granulation, phase  
change, and microstructure. *Chem Phys.* 1941;9:177–84.
28. Flynn JH, Wall LA. A general treatment of the thermogravimetry  
of polymers. *J Res Natl Bur Stand.* 1966;70A:487–523.
29. Yanfen L, Xiaoqian M. Thermogravimetric analysis of the co-  
combustion of coal and paper mill sludge. *Appl Energ.* 2010;  
87:3526–32.
30. Di Nola G, de Jong W, Spliethoff H. TG-FTIR characterization of  
coal and biomass single fuels and blends under slow heating rate  
conditions: partitioning of the fuel-bound nitrogen. *Fuel Process*  
*Technol.* 2010;91:103–15.
31. Shevta G. *Comprehensive analytical chemistry.* In: Shevta G,  
editor. *Analytical infrared spectroscopy, vol. VI.* Amsterdam:  
Elsevier; 1976. pp. 334.
32. Karabakan A, Yürüm Y. Effect of the mineral matrix in the  
reactions of shales. 2. Oxidation reactions of Turkish Göynük and  
U.S. Western Reference shales. *Fuel.* 2000;79:785–92.
33. Pakdel H, Grandmaison JL, Roy C. Analysis of wood vacuum  
pyrolysis solid residues by diffuse reflectance infrared Fourier  
transform spectroscopy. *Can J Chem.* 1989;67:310–4.
34. Pandey KK. Study of the effect of photo-irradiation on the sur-  
face chemistry of wood. *Polym Degrad Stab.* 2005;90:9–20.
35. Bernstein MP, Cruikshank DP, Sandford SA. Near-infrared lab-  
oratory spectra of solid H<sub>2</sub>O/CO<sub>2</sub> and CH<sub>3</sub>OH/CO<sub>2</sub> ice mixtures.  
*Icarus.* 2005;179:527–34.
36. Lemus R. Vibrational excitations in H<sub>2</sub>O in the framework of a  
local model. *J Mol Spectrosc.* 2004;225:73–92.
37. Wu Y-W, Sun S-Q, Zhou Q, Tao J-X, Noda I. Volatility-  
dependent 2D IR correlation analysis of traditional Chinese  
medicine ‘Red Flower Oil’ preparation from different manufactur-  
ers. *J Mol Struct.* 2008;882:107–15.
38. Kök MV. Temperature-controlled combustion and kinetics of  
different rank coal samples. *J Therm Anal Calorim.* 2005;79:  
175–80.
39. Coats AW, Redfern JP. Kinetics parameters from thermogravi-  
metric data. *Nature.* 1964;201:68–9.
40. Otero M, Calvo LF, Gil MV, Garcia AI, Moran A. Co-combus-  
tion of different sewage sludge and coal: a non-isothermal ther-  
mogravimetric kinetic analysis. *Bioresour Technol.* 2008;99:  
6311–9.